On the Role of Line-Edge Roughness on the Diffusion and Localization in GNRs

M. Pourfath*, A. Yazdanpanah†, M. Fathipour†, and H. Kosina*
* Institute for Microelectronics, TU Wien, Gußhausstraße 27–29, 1040 Wien, Austria
†Electrical and Computer Engineering Department, University of Tehran, Tehran, Iran

e-mail: {pourfath|kosina}@iue.tuwien.ac.at

***Abstract*—In this work a comprehensive study of the effect of line-edge roughness on the electronic properties of graphene nanoribbons is presented. The effect of roughness parameters and the role of device geometry is discussed. Depending on these parameters, carrier transport can be in the quasi ballistic, diffusive, or localization regime. Our results show the transport gap of nanoribbons can increase due to the presence of line-edge roughness.**

Graphene, a one-atomic carbon sheet with a honeycomb structure, has attracted significant attention due to its unique physical properties [1]. This material shows an extraordinarily high carrier mobility of more than $100'000\ \mathrm{cm}^2/\mathrm{Vs}$ [2] and is considered a major candidate for a future channel material for high performance transistors [3, 4].

To induce an electronic bandgap, a graphene sheet can be patterned into narrow ribbons [5]. In order to obtain an energy bandgap larger than $0.1\mathrm{eV}$, which is essential for electronic applications, the width of the graphene nanoribbon (GNR) must be scaled below $10\mathrm{nm}$ [6]. In this regime line-edge roughness is the dominant scattering mechanism [7].

Applying a tight-binding model for the electronic structure, the effect of line-edge roughness is studied. We have numerically investigated a large number of different disorder configurations and investigated the diffusive and the localization regime [8]. To model transport of carriers in GNRs the non-equilibrium Green's function (NEGF) formalism is employed. The NEGF method appears to be most appropriate for nanoscale devices [9–13]. This formalism accounts quantum effects such as tunneling, size quantization, and quantum interference of carriers. Quantum mechanical effects in the scattering of carriers, such as collisional energy broadening, are also properly included.

The outline of the paper is as follows. In Section I, the NEGF formalism is briefly described. The implementation of this method for GNRs is presented in Section II. In Section III the role of line-edge roughness is investigated. Finally, the conclusions are presented in Section III-B.

I. Non-equilibrium Green's Function Formalism

The NEGF formalism initiated by Schwinger, Kadanoff, and Baym allows the study of many-particle quantum system. The many-particle information about the system is cast into self-energies, which are part of the equations of motion for the Green's functions. A perturbation expansion of the Green's functions is the key to approximate the self-energies.

Four types of Green's functions are defined as the non-equilibrium statistical ensemble averages of the single particle correlation operator [14]. The greater Green's function $G^{>}$ and the lesser Green's function $G^{<}$ deal with the statistics of carriers. The retarded Green's function G^{R} and the advanced Green's function G^{A} describe the dynamics of carriers.

$$\begin{aligned} G^{>}(1,2) &= -i\hbar^{-1}\langle\hat{\psi}(1)\hat{\psi}^{\dagger}(2)\rangle \\ G^{<}(1,2) &= +i\hbar^{-1}\langle\hat{\psi}^{\dagger}(2)\hat{\psi}(1)\rangle \\ G^{\mathrm{R}}(1,2) &= \theta(t_1-t_2)[G^{>}(1,2)-G^{<}(1,2)] \\ G^{\mathrm{A}}(1,2) &= \theta(t_2-t_1)[G^{<}(1,2)-G^{>}(1,2)] \end{aligned} \tag{1}$$

The abbreviation $1 \equiv (\mathbf{r_1}, t_1)$ is used, $\langle \ldots \rangle$ is the statistical average with respect to the density operator, $\theta(t)$ is the unit step function, $\hat{\psi}^{\dagger}(\mathbf{r_1}, t_1)$ and $\hat{\psi}(\mathbf{r_1}, t_1)$ are the field operators creating or destroying a particle at point $(\mathbf{r_1}, t_1)$ in space-time, respectively. The Green's functions are all correlation functions. For example, $G^{>}$ relates the field operator $\hat{\psi}$ of the particle at point

978-1-4244-9382-1/10/$26.00 ©2010 IEEE

$(\mathbf{r_1}, t_1)$ in space-time to the conjugate field operator $\hat{\psi}^\dagger$ at another point $(\mathbf{r_2}, t_2)$.

Under steady state condition the Green's functions depend only on time differences. One usually Fourier transforms with respect to the time difference coordinate, $\tau = t_1 - t_2$. For example, the lesser Green's function is transformed as $G^<(1,2) \equiv G^<(\mathbf{r_1}, \mathbf{r_2}; E) = \int (d\tau/\hbar) e^{iE\tau/\hbar} G^<(\mathbf{r_1}, \mathbf{r_2}; \tau)$.

Under steady-state condition the equation of motion for the Green's functions can be written as [15]:

$$[E - H]\, G^{\mathrm{R,A}}(1,2) - \int d3 \Sigma^{\mathrm{R,A}}(1,3) G^{\mathrm{R,A}}(3,2) = \delta_{1,2} \tag{2}$$

$$G^{\lessgtr}(1,2) = \int d3 \int d4 G^{\mathrm{R}}(1,3) \Sigma^{\lessgtr}(3,4) G^{\mathrm{A}}(4,2) \tag{3}$$

where H is the single-particle Hamiltonian operator, and Σ^{R}, $\Sigma^<$, and $\Sigma^>$ are the retarded, lesser, and greater self-energies, respectively.

II. Implementation

This section describes the implementation of the NEGF formalism for the numerical analysis of GNRs. A tight-binding Hamiltonian is used to describe the electronic structure in GNRs. The modeling of line-edge roughness is discussed later.

A. Tight-Binding Model

The structure of graphene consists of two types of sublattices A and B, see Fig. 1. In graphene three σ bonds hybridize in an sp^2 configuration, whereas the other $2p_z$ orbital which is perpendicular to the graphene layer, forms π covalent bonds [16]. Each atom in an sp^2-coordination has three nearest neighbors, located $a_{\mathrm{cc}} = 1.42$Å away. It is well known that the electronic and optical properties of carbon nanotubes (CNTs) and GNRs are mainly determined by the π electrons [17]. To model those π electrons, a nearest neighbor tight-binding approximation has been widely used. Using this approximation the Hamiltonian can be written as:

$$H = t \sum_{\langle p,q \rangle} \left(|A_p\rangle\langle B_q| + |B_q\rangle\langle A_p| \right) \ , \tag{4}$$

where $|A_p\rangle$ and $|B_q\rangle$ are the atomic wave functions of the $2p_z$ orbitals which are centered at lattice sites labeled as A_p and B_q, respectively. $\langle p, q\rangle$ represents pairs of nearest neighbor sites p and q, $t = -2.7$ eV is the transfer integral, and the on-site potential is assumed to be zero. For the structure shown in Fig. 1 the matrix elements of the Hamiltonian are non-zero for $p = q$ and $p = q \pm 1$. This atomistic model produces a matrix whose rank is the total

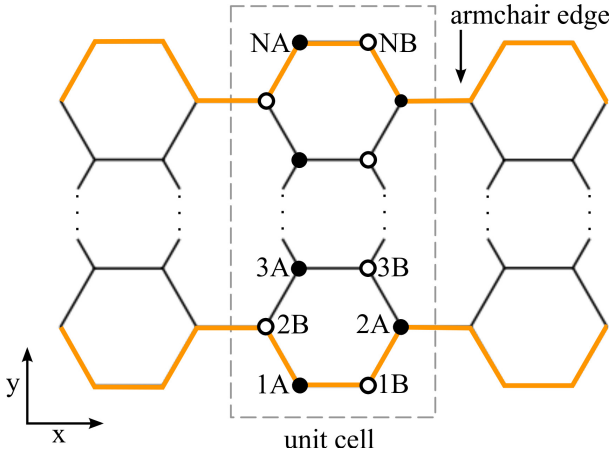

Fig. 1. The structure of a GNR with armchair edges along the transport direction. Each unit cell consists of N numbers of A and B sublattices.

number of carbon atoms [18]. In this method the effect of lattice vacancies [19], roughness [20], impurities [21], and disorder [22] can be rigorously included by changing the hopping parameter at respective atomic sites.

B. Line-Edge Roughness

The line-edge roughness can be treated perturbatively treated [7]. However, in a more accurate non-perturbative approach one can consider the roughness as a stochastic phenomenon and model it by removing or replacing specific carbon atoms located at the edges of the ribbon. In order to model roughness, an exponential auto-correlation function is defined as [23]:

$$c(n) = \Delta_m^2 \exp\left(-\frac{x}{L_m}\right), \quad x = n\Delta x \tag{5}$$

where Δ_m is the roughness amplitude, L_m is the correlation length, and $\Delta x = a_{\mathrm{cc}}/2$ is the sampling interval. The stochastic roughness can be generated by applying a random phase to the power spectrum of the roughness auto-correlation in the Fourier domain and a subsequent inverse Fourier transformation in order to obtain roughness in the real space domain [23].

III. Line-Edge Roughness in GNRs

Fig. 2 shows the spatial distribution of the current amplitude along a GNR with rough edges. The atomistic tight-binding model can capture the granularity of the simulation domain, which is essential for narrow GNRs.

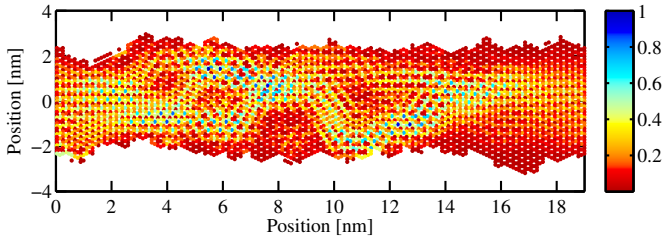

Fig. 2. Spatial distribution of the normalized current amplitude along a GNR with line-edge roughness. The ribbon's length is $L = 19\text{nm}$ and the width $W = 5\text{nm}$. The roughness parameters are $L_m = 3\text{nm}$ and the amplitude $\Delta_m = 0.3\text{nm}$.

A. Quasi Ballistic and Diffusive Transport Regime

Fig. 3 shows the transmission probability, which is averaged over many samples with the same geometrical and roughness parameters, as a function of energy and length of the sample. As this length increases the transmission probability decreases. In the quasi-ballistic and the diffusive regime the average transmission probability $\langle T(E)\rangle$ can be characterized by [15]:

$$\langle T(E)\rangle = \frac{N_{\text{channel}}(E)}{1 + L/\lambda} \tag{6}$$

where $N_{\text{channel}}(E)$ is the number of active subbands (conduction channels) at some energy E, L is the length of the disordered sample, and λ is the mean free path. Fig. 4 shows a fitted curve to the average transmission probability at $E = 0.4\text{eV}$. Fitting Eq. 6 one obtains the elastic mean free path as $\lambda \approx 3\text{nm}$.

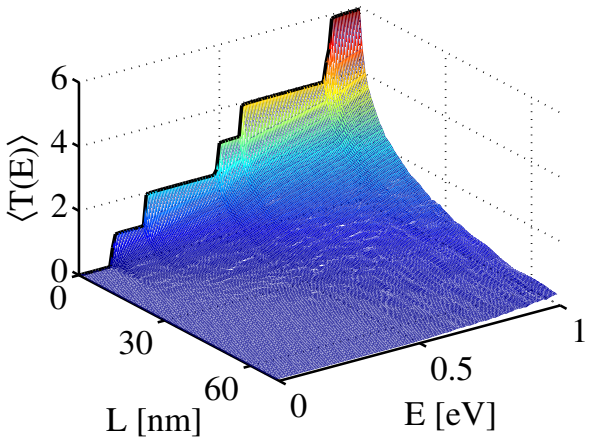

Fig. 3. The average transmission probability as a function of energy and sample length. The solid line at $L = 0$ shows the transmission probability for a perfect GNR. Each peak in the transmission probability denotes the contribution of a new subband. Roughness parameters are $L_m = 3\text{nm}$ and $\Delta_m = 0.3\text{nm}$. The width of all devices is $W = 5\text{nm}$.

B. Localization Regime

For very narrow or very long GNRs line-edge roughness results in the localization of carriers. In this regime, transport takes place by tunneling though localized states and the transmission fluctuates considerably between very small values and values close to 1. In this case, a suitable statistical quantity is provided by $\ln(T(E))$ [8, 15],

$$\langle \ln(T(E))\rangle \propto -L/\xi \tag{7}$$

where ξ is the localization length. In the diffusive regime the resistance increases linearly, whereas in the localization regime it increases exponentially with the length of the device.

Fig. 5 shows a fitted curve to the average of $\ln(T(E))$. Using Eq. 7 the localization length can be estimated as $\xi \approx 6\text{nm}$. It can be shown that the ratio of the localization length to the mean free path is proportional to the number of available subbands: $\xi/\lambda \propto N_{\text{channel}}(E)$. For the discussed sample at $E = 0.4\text{eV}$ this ratio is 2 which is exactly equal to the number of available subbands at this energy. At low energies there are few subbands only and the localization length is short, whereas at higher energies due to the increased number of the subbands the localization length increases. Therefore, the effective transport energy gap increases for GNRs with line-edge roughness. As shown in Fig. 3 the transport gap increases from 0.2eV, for a perfect GNR, to more than 1eV for a GNR with a length of 60nm and given roughness parameters.

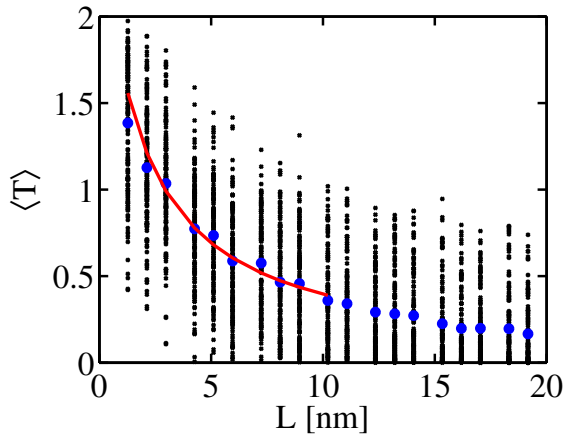

Fig. 4. Small dots show the transmission probability for different samples. The big dots show the average transmission probability over different samples with the same length. The solid line shows the fitted curve to the average transmission probability. $E = 0.4\text{eV}$ and $N_{\text{channel}} = 2$. The extracted mean free path is $\lambda \approx 3\text{nm}$

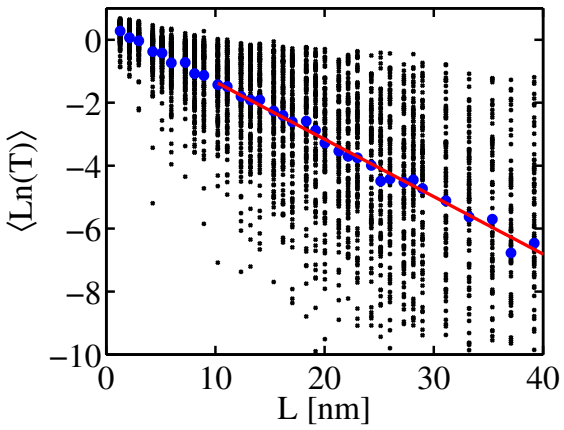

Fig. 5. Small dots show the logarithm of the transmission probability for different samples. The big dots show the average values. The solid line shows the fitted curve to average values. $E = 0.4\text{eV}$ and $N_{\text{channel}} = 2$. The extracted localization length is $\xi = 6\text{nm}$.

CONCLUSIONS

We applied the NEGF formalism to study line-edge roughness in GNRs. An atomistic tight-binding model, which captures the granularity of the simulation domain, has been used. In the presence of line-edge roughness the transport gap of GNRs is found to increase. Our results indicate that in order to employ GNRs for future electronic devices a comprehensive understanding of line edge roughness on the carrier transport properties is required.

ACKNOWLEDGMENT

This work, as part of the ESF EUROCORES program EuroGRAPHENE, was partly supported by funds from FWF, contract I420-N16.

REFERENCES

[1] A.K. Geim and K.S. Novoselov, "The Rise of Graphene," *Nature Mater.*, vol. 6, no. 3, pp. 183–191, 2007.

[2] K.I. Bolotin, , K.J. Sikesb, Z. Jianga, M. Klimac, G. Fudenberga, J. Honec, P. Kima, and H.L. Stormera, "Ultrahigh Electron Mobility in Suspended Graphene," *Solid-State Commun.*, vol. 146, no. 9-10, pp. 351–355, 2008.

[3] Y.-M. Lin, C. Dimitrakopoulos, K. A. Jenkins, D. B. Farmer, H.-Y. Chiu, A. Grill, and P. Avouris, "100-GHz Transistors from Wafer-Scale Epitaxial Graphene," *Science*, vol. 327, no. 5966, pp. 661, 2010.

[4] F. Xia, D. B. Farmer, Y Lin, and P. Avouris, "Graphene Field-Effect Transistors with High On/Off Current Ratio and Large Transport Band Gap at Room Temperature," *Nano Lett.*, vol. 10, no. 2, pp. 715–718, 2010.

[5] C. Berger, Z. Song, X. Li, X. Wu, N. Brown, C. Naud, D. Mayou, T. Li, J. Hass, A.N. Marchenkov, E.H. Conrad, P.N. First, and W.A. de Herr, "Electronic Confinement and Coherence in Patterned Epitaxial Graphene," *Science*, vol. 312, no. 5777, pp. 1191–1196, 2006.

[6] M.Y. Han, B. Özyilmaz, Y. Zhang, and P. Kim, "Energy Band-Gap Engineering of Graphene Nanoribbons," *Phys. Rev. Lett.*, vol. 98, no. 20, pp. 206805 (4pp), 2007.

[7] T. Fang, A. Konar, H. Xingi, and D. Jena, "Mobility in Semiconducting Graphene Nanoribbons: Phonon, Impurity, and Edge Roughness Scattering," *Phys. Rev. B*, vol. 78, no. 20, pp. 205403 (8pp), 2008.

[8] A. Cresti and S. Roche, "Range and Correlation Effects in the Edge Disordered Graphene Nanoribbons," *New J. Phys.*, vol. 11, pp. 095004 (12pp), 2009.

[9] A. Svizhenko, M. P. Anantram, T. R Govindan, B. Biegel, and R. Venugopal, "Two-Dimensional Quantum Mechanical Modeling of Nanotransistors," *J. Appl. Phys.*, vol. 91, no. 4, pp. 2343–2354, 2002.

[10] J. Guo, "A Quantum-Mechanical Treatment of Phonon Scattering in Carbon Nanotube Transistors," *J. Appl. Phys.*, vol. 98, pp. 063519, 2005.

[11] A. Svizhenko, M. P. Anantram, and T. R. Govindan, "Ballistic Transport and Electrostatics in Metallic Carbon Nanotubes," *IEEE Trans. Nanotechnol.*, vol. 4, no. 5, pp. 557–562, 2005.

[12] M. Pourfath and H. Kosina, "The Effect of Phonon Scattering on the Switching Response of Carbon Nanotube FETs," *Nanotechnology*, vol. 18, pp. 424036–6, 2007.

[13] G. Klimeck, S. S. Ahmed, N. Kharche, M. Korkusinski, M. Usman, M. Prada, and T. B. Boykin, "Atomistic Simulation of Realistically Sized Nanodevices Using NEMO 3-D Part I: Models and Benchmarks," *IEEE Trans. Electron Devices*, vol. 54, no. 9, pp. 2079–2089, 2007.

[14] G. D. Mahan, *Many-Particle Physics*, Physics of Solids and Liquids. Plenum Press, New York, 2nd edition, 1990.

[15] S. Datta, *Electronic Transport in Mesoscopic Systems*, Cambridge University Press, New York, 1995.

[16] R. Saito, G.D. Dresselhaus, and M.S. Dresselhaus, *Physical Properties of Carbon Nanotubes*, Imperial College Press, London, 1998.

[17] Y.-W. Son, M.L. Cohen, and S.G. Louie, "Half-Metallic Graphene Nanoribbons," *Nature (London)*, vol. 444, no. 7117, pp. 347–349, 2006.

[18] J. Guo, S. Datta, M. Lundstrom, and M.P. Anantram, "Multi-Scale Modeling of Carbon Nanotube Transistors," *Intl. J. Multiscale Comput. Eng.*, vol. 2, no. 2, pp. 257–278, 2004.

[19] Y. Yoon, G. Fiori, S. Hong G. Iannaccone, and J. Guo, "Performance Comparison of Graphene Nanoribbon FETs With Schottky Contacts and Doped Reservoirs," *IEEE Trans. Electron Devices*, vol. 55, no. 9, pp. 2314–2323, 2009.

[20] Y. Yoon and J. Guo, "Effect of Edge Roughness in Graphene Nanoribbon Transistors," *Appl. Phys. Lett.*, vol. 91, no. 7, pp. 073103 (3pp), 2007.

[21] N. Neophytou, D. Kienle, E. Polizzi, and M. P. Anantram, "Influence of Defects on Nanotube Transistor Performance," *Appl. Phys. Lett.*, vol. 88, pp. 242106 (3pp), 2006.

[22] X. Ni, G. Liang, J.-S. Wang, and B. Li, "Disorder Enhances Thermoelectric Figure of Merit in Armchair Graphane Nanoribbons," *Appl. Phys. Lett.*, vol. 95, pp. 192114 (3pp), 2009.

[23] S. M. Goodnick, D. K. Ferry, C. W. Wilmsen, Z. Liliental, D. Fathy, and O. L. Krivanek, "Surface roughness at the Si(100)-$SiO2$ interface," *Phys. Rev. B*, vol. 33, no. 12, pp. 8171–8186, 1985.